

# UC Berkeley

## UC Berkeley Previously Published Works

### Title

Reducing conditions, reactive metals, and their interactions can explain spatial patterns of surface soil carbon in a humid tropical forest

### Permalink

<https://escholarship.org/uc/item/5hm02643>

### Journal

Biogeochemistry, 125(2)

### ISSN

0168-2563

### Authors

Hall, Steven J  
Silver, Whendee L

### Publication Date

2015-09-01

### DOI

10.1007/s10533-015-0120-5

Peer reviewed

# Reducing conditions, reactive metals, and their interactions can explain spatial patterns of surface soil carbon in a humid tropical forest

- [Authors](#)
  - [Authors and affiliations](#)
- 

- Steven J. Hall
- Whendee L. Silver

## Abstract

Humid tropical forests support large stocks of surface soil carbon (C) that exhibit high spatial variability over scales of meters to landscapes (km). Reactive minerals and organo-metal complexes are known to contribute to C accumulation in these ecosystems, although potential interactions with environmental factors such as oxygen (O<sub>2</sub>) availability have received much less attention. Reducing conditions can potentially contribute to C accumulation, yet anaerobic metabolic processes such as iron (Fe) reduction can also drive substantial C losses. We tested whether these factors could explain variation in soil C (0–10 and 10–20 cm depths) over multiple spatial scales in the Luquillo Experimental Forest, Puerto Rico, using reduced iron (Fe(II)) concentrations as an index of reducing conditions across sites differing in vegetation, topographic position, and/or climate. Fine root biomass and Fe(II) were the best overall correlates of site (n = 6) mean C concentrations and stocks from 0 to 20 cm depth (r = 0.99 and 0.98, respectively). Litterfall decreased as reducing conditions, total and dead fine root biomass, and soil C increased among sites, suggesting that decomposition rates rather than C inputs regulated soil C content at the landscape scale. Strong relationships between Fe(II) and dead fine root biomass suggest that reducing conditions suppressed particulate organic matter decomposition. The optimal mixed-effects regression model for individual soil samples (n = 149) showed that aluminum (Al) and Fe in citrate/ascorbate and oxalate extractions, Fe(II), fine root biomass, and interactions between Fe(II) and Al explained most of the variation in C concentrations (pseudo R<sup>2</sup> = 0.82). The optimal model of C stocks was similar but did not include fine root biomass (pseudo R<sup>2</sup> = 0.62). In these models, soil C concentrations and stocks increased with citrate/ascorbate-extractable Al and oxalate-extractable Fe. However, soil C decreased with citrate/ascorbate-extractable Fe, an index of Fe susceptible to anaerobic microbial reduction. At the site scale (n = 6), ratios of citrate/ascorbate to

oxalate-extractable Fe consistently decreased across a landscape O<sub>2</sub> gradient as C increased. We suggest that the impact of reducing conditions on organic matter decomposition and the presence of organo-metal complexes and C sorption by short-range order Fe and Al contribute to C accumulation, whereas the availability of an Fe pool to sustain anaerobic respiration in soil microsites partially attenuates soil C accumulation in these ecosystems.

## Keywords

Iron reduction Poorly-crystalline minerals Redox Root biomass Soil carbon Soil oxygen

Responsible Editor: Kate Lajtha.

## Electronic supplementary material

The online version of this article (doi: [10.1007/s10533-015-0120-5](https://doi.org/10.1007/s10533-015-0120-5)) contains supplementary material, which is available to authorized users.

## Introduction

Identifying the mechanisms underlying the accumulation and distribution of soil C in humid tropical forests represents an important challenge given their large soil C stock (~500 Pg), rapid decomposition rates, and potentially large feedbacks to global climate change (Jobbagy and Jackson [2000](#); Malhi and Grace [2000](#); Parton et al. [2007](#)). Numerous studies have demonstrated the importance of short-range order and monomeric Al and Fe in protecting organic matter from microbial decomposition due to mineral sorption and the precipitation of organo-metal complexes (e.g. Baldock and Skjemstad [2000](#); Kaiser and Guggenberger [2000](#); Wagai and Mayer [2007](#)). Accordingly, increasing concentrations of short-range order minerals or poorly-crystalline Fe and Al measured in chemical extractions have often correlated with decreased decomposition rates and increased C concentrations across a broad spectrum of temperate and tropical ecosystems (Torn et al. [1997](#); Kleber et al. [2005](#); Bruun et al. [2010](#); Kramer et al. [2012](#)). In wet ecosystems characteristic of the humid tropics, variation in soil O<sub>2</sub> availability and the consequent prevalence of hypoxia or reducing conditions can also significantly impact surface soil C cycling (Silver et al. [1999](#); Schuur [2001](#); Schuur et al. [2001](#); Liptzin et al. [2011](#)), but these mechanisms have received little attention in comparison with short-range order minerals and metals. Importantly, soil O<sub>2</sub> concentrations are closely linked with climate via precipitation and temperature patterns at landscape scales (Silver et al. [1999](#), [2013](#)), thus providing a potential mechanistic linkage between spatial and temporal variation in climate and soil C stocks that could be included in process-based models. Here, we tested whether multiple indices of reactive Fe and Al, reducing conditions, and their

interactions could explain the distribution of surface soil C (0–10 and 10–20 cm depth increments) over coarse and fine spatial scales across a humid tropical forest landscape. We define reactive Fe and Al pools operationally in terms of multiple chemical extractions used in this study, which are explained in detail in the Methods.

Humid tropical forests often experience a combination of high precipitation, temperature, and soil respiration that generates periodic oxygen (O<sub>2</sub>) limitation in surface soils at scales of microsites to entire soil profiles (Silver et al. [1999](#); Schuur et al. [2001](#); Cleveland et al. [2010](#); Liptzin et al. [2011](#); Silver et al. [2013](#); Hall et al. [2013](#)). Soil O<sub>2</sub> availability and the prevalence of reducing microsites vary with precipitation, soil moisture, and soil texture and structure, which control diffusive O<sub>2</sub> supply to the soil profile, as well as heterotrophic and autotrophic respiration, which control rates of O<sub>2</sub> consumption. Anaerobic conditions are well known to constrain organic matter decomposition in flooded wetland ecosystems (Ponnamperuma [1972](#)), but the potential influence of O<sub>2</sub> limitation on C accumulation in terrestrial soils has received less attention. Soil C stocks increased monotonically with decreasing redox potential across a precipitation gradient in Hawaii even as plant productivity declined, suggesting that reducing conditions promoted soil C accumulation at the landscape scale (Schuur et al. [2001](#)). Concentrations of short-range order minerals declined with increasing precipitation along the same gradient, implying that anaerobic constraints on decomposition as opposed to organo-mineral interactions were primarily responsible for increased C accumulation (*ibid.*). Soil C concentrations and stocks increased with elevation in New Guinean and Puerto Rican humid tropical forests, although relationships with short-range order minerals and reducing conditions were not quantified (McGroddy and Silver [2000](#); Dieleman et al. [2013](#)).

Understanding the potentially nuanced interactions between O<sub>2</sub> availability and reactive metals could provide additional insight into spatial patterns of C in humid tropical forest soils. In particular, impacts of reducing conditions on soil C storage may depend on multiple additional factors related to Fe and Al speciation and concentrations. Previous research examining organo-mineral interactions in upland soils has largely emphasized the capacity of Fe oxides to protect C from decomposition via sorption and complexation (e.g. Kleber et al. [2005](#); Wagai and Mayer [2007](#)), with less emphasis on their capacity to facilitate C loss during anaerobic respiration (Peretyazhko and Sposito [2005](#)). Although the anaerobic metabolic process of dissimilatory Fe reduction has primarily been studied in submerged sediments, it has been shown to sustain high rates of microbial respiration in surface horizons of terrestrial humid tropical soils, where densities of Fe reducing bacteria can exceed those of submerged sediments (Chacón et al. [2006](#); Thompson et al. [2006](#); Dubinsky et al. [2010](#)). Rates of CO<sub>2</sub> production from Fe reduction can

be highly significant: anaerobic respiration rates from a tropical Ultisol measured 70–100 % of aerobic controls over short-term incubations (McNicol and Silver [2014](#)). Although short-range order Fe oxides are often abundant in humid tropical soils, they can eventually be depleted by reduction and leaching over pedogenic timescales (Thompson et al. [2011](#)), which could ultimately limit the overall importance of Fe reduction and contribute to soil C accumulation.

To evaluate relationships between reducing conditions, reactive minerals/metals, and soil C, we collected 149 soil samples from six sites encompassing variation in soil O<sub>2</sub> dynamics driven by topography and climate. At landscape scales, biological factors affecting C inputs likely co-vary with physical and geochemical factors affecting C accumulation. Therefore, we also report litterfall productivity (NPP) at the site scale, and report fine root biomass at the scale of individual soil samples. Although fine root biomass is not an effective proxy for root productivity, it can provide an index of the decomposition rates of particulate organic matter, relative patterns of belowground C allocation, and/or nutrient limitation (Vogt et al. [1996](#); Ostertag [2001](#); Espeleta and Clark [2007](#)). These factors are important given that fine roots represent a dominant source of soil C (Rasse et al. [2005](#)). Furthermore, fine roots can be assayed at the same fine spatial scales (cm) as soil chemical constituents and C concentrations, yet few studies of fine roots have been combined with high-resolution measurements of soil C within ecosystems (Vogt et al. [1996](#)). The majority of samples (n = 119) in this study were collected from four replicate catenas in a lower montane forest that experienced similar climate, and also from three other montane sites (n = 30) characterized by higher rainfall and slightly lower temperatures. Previous work showed that mineral-associated as opposed to particulate C is dominant in the lower montane sites and at least one of the montane sites, accounting for 75–90 % of total C in surface horizons on a mass basis (Cusack et al. [2011](#); Hall et al. [2015a, b](#)). However, particulate C is increasingly important in the two highest-elevation sites (McGroddy and Silver [2000](#)). In particular, we sought to address the relative importance of reducing conditions, fine roots, and multiple reactive Al and Fe fractions as potential mechanisms associated with C accumulation.

## Methods

### Site description

We sampled soils from the Luquillo Experimental Forest, Puerto Rico, an NSF-funded Long Term Ecological Research and Critical Zone Observatory site (Table [1](#)). We intensively sampled four ridge/slope/valley catenas in a lower montane (200–300 masl) forest in the Bisley watersheds, and we sampled ridge positions in three higher-elevation montane forests at 610, 740, and 940 masl, respectively. We emphasize that because we sampled

four separate catenas in the lower montane forest, our data can be considered broadly representative of that forest type. For the montane forest sites, our data are representative of the selected sites (due to random selection of sampling plots), but not the forest types as a whole due to the lack of site replication. Rather, sites were selected because of their position on a climate/soil O<sub>2</sub> gradient, detailed below (Silver et al. [1999](#), [2013](#)).

**Table 1**

Site characteristics

| Site                   | Elevation (m) | N (°)       | W (°)       | Total aboveground litterfall (g m <sup>-2</sup> year <sup>-1</sup> ) |
|------------------------|---------------|-------------|-------------|--|
| Bisley ridges (n = 4)  | 240-300       | 18.315<br>7 | 65.748<br>7 | 870 (70)   |
| Bisley slopes (n = 4)  | 220-280       | -           | -           | -  |
| Bisley valleys (n = 4) | 210-240       | -           | -           | -  |
| Palm                   | 614           | 18.298<br>8 | 65.780<br>3 | 470 (107)  |
| Palo colorado          | 736           | 18.294<br>2 | 65.785<br>2 | 560 (90)   |
| Elfin                  | 936           | 18.270<br>2 | 65.761      | 366 (55)   |

Above-ground litterfall represents annual means (SE) from 1994–2002 from the palm, palo colorado, and elfin sites, based on monthly litter collection from five replicate baskets per site (W. Silver, unpublished data). Bisley (lower montane forest) data represent bi-weekly litter collections from 60 baskets for 18 months in 1988–89, spanning ridge, slope, and valley positions (Scatena et al. [1996](#)). Bisley litterfall NPP was similar among topographic positions (US Forest Service International Institute for Tropical Forestry, unpublished data)

The Bisley watershed is described locally as a tabonuco forest after the dominant species, *Dacryodes excelsa* Vahl, and supports 127 shrub and tree species (Chinea et al. [1994](#)). Together, *D. excelsa*, *Sloanea berteriana* Choisy ex. DC, and *Prestoea acuminata* (Willd.) H.E. Moore var. *montana* (Graham) A. Hend. & G. Galeano, known locally as sierra palm, comprised approximately 60 % of total aboveground biomass (Scatena and Lugo [1995](#)). Species composition varies with topographic position, and Heartsill-Scalley et al. ([2010](#)) provide a detailed description of spatial and temporal

vegetation trends in this forest. Aboveground biomass also varied strongly with topographic position, decreasing from  $360 \pm 60 \text{ Mg Ha}^{-1}$  on ridges to  $190 \pm 30$  and  $120 \pm 60 \text{ Mg Ha}^{-1}$  in valleys (Scatena and Lugo 1995). However, litterfall NPP was statistically similar among topographic positions (US Forest Service International Institute for Tropical Forestry, unpublished data). Understory vegetation was sparse in all sites sampled here.

The forested site at 610 m was dominated by sierra palm, the 740 m site by palo colorado (*Cyrilla racemiflora* L.), and the 940 m site supported a cloud forest dominated by *Tabebuia rigida* Urb. The latter species typically comprises more than 50 % of tree basal area in these communities, which are locally described and referred to here as “elfin forests” due to their stunted vegetation canopy (Weaver et al. 1986). The frequent presence of fog, low soil O<sub>2</sub> availability, and high winds likely constrain NPP in the elfin forest relative to the other sites sampled here. Aboveground litterfall was greatest in the lower montane forest, intermediate in the sierra palm and palo colorado sites, and lowest in the elfin forest site (Table 1). We note that litterfall measurements reflect means from multiple litter baskets distributed within the sites, and thus could not be included in mixed-effects models of soil C at the finer spatial scales of individual soil samples. Litter decomposition rates are extremely rapid in the lower montane forest, with mean residence times of 0.8 and 0.9 y for leaves and roots, respectively (Cusack et al. 2009). Litter decomposition rates were lower in the palo colorado and elfin forests, where a separate study measured mean litter residence times of 1.1 and 2.7 year, respectively (DeAngelis et al. 2013).

Soils in these forests are largely derived from andesitic to basaltic volcanoclastic sedimentary rocks, with a likely contribution from quartz diorite in the palo colorado site. In the lower montane forest, soils on stable ridges are dominantly Ultisols (Typic Haplohumults), slopes are Oxisols (Inceptic and Aquic Hapludox), and valleys are Inceptisols (Typic Eutrudepts; Soil Survey Staff 2002). In the montane sites, palm forest soils are Inceptisols (Aquandic Humaquepts), and palo colorado and elfin forest soils are Oxisols (Humic Haplaquox). The lower montane forest received a long-term mean annual precipitation of  $3800 \text{ mm year}^{-1}$ , which varied between  $2600$  and  $5800 \text{ mm year}^{-1}$  from 1989 to 2011 (<http://criticalzone.org/luquillo/data/dataset/2403/>). Mean annual precipitation increases with elevation in the Luquillo Mountains and measures approximately  $4500 \text{ mm year}^{-1}$  in the elfin forest (McDowell et al. 2012), although additional inputs from horizontal precipitation, fog, and cloud-water inputs are important but difficult to quantify. Precipitation is relatively aseasonal, as even the driest months (January and February) receive mean rainfall of 190 and 180 mm, respectively. Mean annual temperature measures  $24 \text{ }^{\circ}\text{C}$  in the lower montane forest and decreases with elevation to  $20 \text{ }^{\circ}\text{C}$  in the elfin forest with little intra-annual variability



(McDowell et al. [2012](#)). Precipitation and temperature in the sierra palm and palo colorado sites are intermediate between the elfin and the lower montane sites. These sites are frequently impacted by hurricanes, although storms do not have a discernable short-term impact on soil C as evidenced by repeated measurements over a decade that included multiple hurricanes (Teh et al. [2009](#)).

These forested sites represent a gradient in soil O<sub>2</sub> concentrations, measured in gas equilibration chambers (10 cm depth) over multiple years (Silver et al. [1999](#), [2013](#)). Mean soil O<sub>2</sub> decreased from ridges to slopes to riparian valleys in the lower montane forest (19, 16, and 11 % O<sub>2</sub>), respectively, with the riparian valleys experiencing frequent low O<sub>2</sub> events (<3 %). Mean O<sub>2</sub> decreased further as elevation increased from the sierra palm to palo colorado to elfin forest sites, measuring approximately 10, 9, and 8 % O<sub>2</sub>, respectively; similarly, these sites were characterized by frequent periods of O<sub>2</sub> concentrations <3 %. Elevated methane concentrations indicate the presence of anaerobic microsites (Silver et al. [1999](#)). Because Fe oxides represent the most abundant anaerobic terminal electron acceptor in these soils (Hall et al. [2013](#)), we used measurements of Fe(II) (described below) to provide an index of reducing conditions at the scale of individual soil samples. Previous studies have often used redox potential measurements (Eh) to characterize reducing conditions in soil microsites. However, Eh measurements are highly spatially variable and are difficult to compare among soils (Christensen et al. [2000](#)). In contrast, measurements of Fe(II) and Fe(III) in soil extractions are quantitative, chemically meaningful, and integrate a defined soil volume.

## Soil sampling and analysis

In the lower montane forest, we sampled four catenas in June 2011 that each consisted of a ridge, slope, and riparian valley. We randomly located five plots (0.25 m<sup>2</sup>) in each topographic zone in each catena, along 50 m linear transects at 5–10 m intervals. We similarly sampled transects in ridge positions of the montane forest sites (one transect per site) in February 2012, yielding a total of 119 samples from the lower montane forest (rocks prevented collection of one sample) and 30 samples from the montane forest sites (total n = 149). In each plot, we collected four replicate 6-cm diameter soil cores (volume = 283 cm<sup>3</sup>) at depths of 0–10 cm and 10–20 cm, where root biomass and organic matter are most abundant in these forests (Silver and Vogt [1993](#)). Recognizable surface litter (Oi horizon material) was carefully removed where present prior to soil sampling. Accumulated surface litter tends to be sparse and discontinuous in the lower montane sites and slightly greater in the montane sites, and represents <5 % of total soil C to 20 cm (Johnson et al. [2015](#)). The 0–10 cm increment corresponded closely with the depth of the A horizon in most plots, whereas the 10–20 cm



increment typically represented the upper portion of a Bt horizon. Representative soil pits in a lower montane ridge, slope, and valley had A horizons at depths of 0–10, 0–9, and 0–10 cm, and B1 horizons at depths of 10–22, 9–25, and 10–20 cm, respectively. Soil depth did not exceed 20 cm in some riparian valley plots due to the presence of buried boulders. Thus, we sampled common depth intervals present in all plots. We note that 0–10 cm samples from the palm forest had extremely low bulk density, although samples were clearly differentiated from surface litter by the presence of mineral soil aggregation. In the elfin forest, we avoided sampling soils immediately adjacent to woody superficial roots, which are common in this forest type.

We used four separate soil extraction protocols that provide different operationally defined indices of reactive Fe and Al, described below and in Table 2. Wagai et al. (2011) further discuss several of these extraction methods. Two cores from each depth were immediately composited and homogenized, and separate subsamples were extracted in solutions of 0.5 M hydrochloric acid (HCl) and 0.2 M sodium citrate/0.05 M ascorbic acid within 1 min of sampling. The HCl extraction solubilizes adsorbed and some solid phase Fe(II), and a reactive fraction of Fe(III) minerals (Fredrickson et al. 1998). The low pH of the HCl solution inhibits Fe(II) oxidation prior to analysis. Soil subsamples (3 g dry mass equivalent) were immersed in a 1:10 ratio with HCl, vortexed, shaken for 1 h, and filtered to 0.22  $\mu\text{m}$ . We measured concentrations of Fe(II) and Fe(III) colorimetrically using a ferrozine assay (Viollier et al. 2000). We subsequently used Fe(II) concentrations and the ratio of Fe(II) to total Fe in the HCl extraction ( $\text{Fe(II)}/\text{Fe}_{\text{HCl}}$ ) as indices of reducing conditions. Normalizing Fe(II) concentrations by the total  $\text{Fe}_{\text{HCl}}$  pool yields the fraction of the  $\text{Fe}_{\text{HCl}}$  pool that is reduced, thus accounting for differences in  $\text{Fe}_{\text{HCl}}$  among samples. To further assess temporal variation in Fe(II) within and among catena positions, additional soils were collected in February and May 2012 from one of the catenas described above (15 plots  $\times$  two depth increments) at locations within 0.5 m of the original samples, and were extracted in 0.5 M HCl.

**Table 2**

Potential predictors of soil C concentrations and stocks in mixed-effects models

| Variable                | Description                      | Interpretation   |
|-------------------------|----------------------------------|--|
| $\text{Fe}_{\text{ca}}$ | Citrate/ascorbate-extractable Fe | Reducible short-range order (oxy)hydroxides and organo-Fe complexes                      |
| $\text{Al}_{\text{ca}}$ | Citrate/ascorbate-extractable Al | Al substituted in reducible short-range order Fe (oxy)hydroxides and organo-Al complexes |

| Variable                 | Description   | Interpretation   |
|--------------------------|---|--|
| Fe <sub>ox</sub>         | Ammonium oxalate-extractable Fe                             | Chelatable short-range order (oxy)hydroxides and organo-Fe complexes |
| Al <sub>ox</sub>         | Ammonium oxalate-extractable Al                             | Chelatable short-range order (oxy)hydroxides and organo-Al complexes |
| Fe(III) <sub>HCl</sub>   | Fe(III) in 0.5 M HCl  | Weak acid soluble short-range order and organo-Fe complexes          |
| Al <sub>HCl</sub>        | Al in 0.5 M HCl   | Weak acid soluble short-range order and organo-Al complexes          |
| Fe(II)/Fe <sub>HCl</sub> | Ratio of Fe(II) to total Fe in 0.5 M HCl                    | Weak acid soluble Fe(II) normalized by Fe <sub>HCl</sub>             |
| Fe <sub>cd</sub>         | Fe in citrate/dithionite extractions                        | Total free Fe oxides (crystalline and short-range order)             |
| Fe <sub>cd-ca</sub>      | Fe in citrate/dithionite extractions minus Fe <sub>ca</sub> | Crystalline Fe oxides (e.g. goethite and hematite)                   |
| Fine roots               | Roots ≤2 mm   | Live + dead fine roots   |
| Depth                    | 0-10 and 10-20 cm increments                                |  |
| Clay                     | Particles <2 μm   |  |
| Sand                     | Particles 50-2000 μm  |  |
| Silt                     | Particles 2-50 μm   |  |

Citrate/ascorbate and HCl extractions were conducted on moist soils in the field, and the other extractions were conducted on air-dried soils. See “[Soil sampling and analysis](#)” section for details of soil analyses

We also extracted soils with sodium citrate/ascorbate solution (Reyes and Torrent [1997](#)) to provide an estimate of reducible Fe oxides (Fe<sub>ca</sub>). This assay reductively dissolves and chelates Fe oxides in proportion to a pool that is potentially reducible by microbes (Hyacinthe et al. [2006](#)). Soil subsamples (1.5 g dry mass equivalent) were combined in a 1:30 ratio with citrate/ascorbate solution in the field, vortexed and then shaken for 18 h, and centrifuged for 10 min at 1500 rcf. We additionally extracted separate soil subsamples with acid ammonium oxalate solution in the dark at pH 3 (Loeppert and Inskeep [1996](#)) to provide a separate index of chelatable Fe

and Al ( $\text{Fe}_{\text{ox}}$  and  $\text{Al}_{\text{ox}}$ ), omitting removal of carbonates, which are negligible in these soils. Oxalate-extractable metals have been defined as “poorly crystalline” forms in previous studies (Torn et al. [1997](#); Kleber et al. [2005](#)). This pool may differ subtly from citrate/ascorbate Fe, which reflects Fe solubilized via reductive dissolution and includes a smaller fraction of Fe chelatable by citrate alone. Citrate/ascorbate solution is advantageous as it does not appear to solubilize crystalline minerals (Reyes and Torrent [1997](#)). We used air-dried and ground samples for the oxalate extraction for best comparison with previously published results, and because oxalate can extract crystalline Fe in the presence of Fe(II), which persists in moist soils (Phillips et al. [1993](#)). We note that trends and relative differences in metal concentrations among these extractions are likely to be more meaningful than differences in their absolute magnitude, given that citrate/ascorbate extractions were conducted on field-moist samples whereas oxalate extractions were conducted on air-dried samples according to standard protocols (Loeppert and Inskeep [1996](#)). Our field extractions with citrate/ascorbate are perhaps best representative of the in situ concentrations of short-range order Fe minerals and associated/substituted Al, as well as Fe and Al in organic complexes. Citrate/ascorbate extractions of field-moist soils (Dubinsky et al. [2010](#)) yielded much higher Fe concentrations than air-dried soils (Reyes and Torrent [1997](#)), presumably due to mineral crystallization. We did not use a sodium pyrophosphate extraction in this study because recent work suggests that much of the Fe solubilized by this method represents nano-crystalline phases rather than organo-Fe complexes (Thompson et al. [2011](#)). We would also expect this nano-crystalline Fe to also contain co-precipitated Al.

Air-dried and ground subsamples were also extracted with sodium citrate/dithionite solution (Loeppert and Inskeep [1996](#)) to measure total free Fe oxides ( $\text{Fe}_{\text{cd}}$ ). Dithionite is a stronger reductant than ascorbate and dissolves crystalline Fe minerals such as goethite and hematite. Thus, Fe extracted by citrate/dithionite spans crystalline to poorly-crystalline phases, overlapping the pool extracted by citrate/ascorbate. We estimated the pool of crystalline Fe extractable by citrate/dithionite but not citrate/ascorbate as the difference between these extractions ( $\text{Fe}_{\text{cd-ca}}$ ). Iron and Al in soil extractions were analyzed in triplicate via inductively coupled plasma optical emission spectrometry (ICP-OES; Perkin Elmer Optima 5300 DV, Waltham, Massachusetts). Concentrations of  $\text{Fe}_{\text{HCl}}$  determined colorimetrically and via ICP-OES agreed to within 1 %. Soil subsamples for C analysis were air dried and sieved to 2 mm, and visible roots were removed by hand. Samples were ground to a fine powder and analyzed in duplicate for total C by combustion on a CE Elantech elemental analyzer (Lakewood, NJ). Duplicate samples differed by an average of 2 %. Soil C content was corrected for any moisture remaining (0.5–2 %) after drying at 105 °C.

The two remaining 6 cm diameter cores from each plot and depth (sample volume = 283 cm<sup>3</sup>, total n = 149) were assayed for root biomass and bulk density, respectively. All cores were sampled quantitatively in 10-cm increments, and no sample compression was evident. Cores for root biomass analysis were sieved with water, and fine roots ( $\leq 2$  mm diameter) were separated into live and dead fractions based on turgor, tensile strength, and integrity of the stele tissue (Silver and Vogt [1993](#)). Roots were thoroughly rinsed in deionized water and dried at 65 °C to constant mass. Bulk density was determined gravimetrically on a separate replicate 6-cm diameter core after correcting for the volume of any rocks (diameter >2 mm) or coarse roots (diameter >5 mm), which had a minimal effect (2 %) on bulk density measurements. Soils were dried at 105 °C to constant mass, and bulk density was calculated as dry soil mass divided by the corrected sample volume. We analyzed additional subsamples of field-moist soil from each plot for particle size using the hydrometer method (Gee and Bauder [1986](#)). Organic matter was not removed prior to texture analysis. Samples (50 g dry mass equivalent) were passed through a 2 mm sieve, soaked for 16 h in 50 g l<sup>-1</sup> sodium hexametaphosphate solution, and dispersed in an electric mixer. We measured changes in soil suspension density over 24 h to calculate clay, sand, and silt fractions.

## Statistical analysis

We compared site means (n = 6) of soil C and other biogeochemical variables with linear models where variances were allowed to vary among sites using the `gls` function in R (Pinheiro et al. [2014](#)), with post hoc comparisons using Tukey's honestly significant difference test. Pairwise relationships among site mean values were assessed using Pearson correlation coefficients. We did not include litterfall NPP in correlation analyses because values were equivalent for different topographic positions in the lower montane forest, resulting in only four independent measurements (lower montane, palo colorado, sierra palm, elfin). We note that because the montane forest soil analyses were not replicated at different sites within a given forest type, statistical comparisons are restricted to these particular sites, and cannot be generalized to the forest types as a whole.

Relationships between soil C and predictor variables at the scale of individual soil samples (n = 149) were analyzed using linear mixed-effects regression models fit using the `lme` function in R (Pinheiro et al. [2014](#)). Soil C concentrations and stocks were modeled separately. Models included transects and plots as random effects to account for the spatial structure of our sampling design (samples within plots within sites), thus avoiding pseudoreplication. All of the variables listed in Table [2](#) were included as potential predictors during model selection. Depth was necessarily included

as a blocking factor to account for the structure of the sampling design and any depth-related variation in C not explained by the other predictor variables. We also included interaction terms between  $Al_{ca}$  and  $Fe(II)/Fe_{HCl}$ , and  $Fe_{ca}$  and  $Fe(II)/Fe_{HCl}$  as potential predictors given the possibility of interactions between reducing conditions and short-range order Fe and Al as discussed in the Introduction. Predictor variables were normalized by mean and standard deviation to allow comparisons of variable importance analogous to Pearson's  $r$ . We selected the optimal combination of fixed-effect predictors using stepwise backwards elimination from a model including all potential predictors, using  $p < 0.01$  as the significance criterion. We fit separate models for two datasets: the lower montane soils ( $n = 119$ ), given that they comprised the majority of our samples and experienced a relatively uniform climate, and the lower montane and the montane soils together ( $n = 149$ ). Two outliers with extremely high  $Fe(II)$  concentrations were removed from this analysis. Variance inflation and model matrix condition numbers implied that multicollinearity among variables was unimportant. We present pseudo- $R^2$  values, which correct for the presence of random effects in the models (Nakagawa and Schielzeth [2013](#)).

## Results

### Landscape patterns of soil carbon concentrations, stocks, and covariates

Mean C concentrations differed significantly among sites and topographic positions, but were not significantly correlated with long-term mean soil  $O_2$  concentrations at the site scale (Fig. [1a](#), Supplemental Table 1). Rather, variation in mean site soil C concentrations (0–20 cm,  $n = 6$  sites) correlated most strongly with total fine root biomass ( $r = 0.99$ ,  $p < 0.001$ ; Supplemental Table 1) and an index of reducing conditions,  $Fe(II)$  ( $r = 0.94$ ,  $p < 0.01$ ). Similarly, the strongest predictors of mean site soil C stocks were total and dead fine root biomass ( $r = 0.99$ ,  $p < 0.001$  for both variables), and  $Fe(II)$  ( $r = 0.98$ ,  $p < 0.001$ ). Concentrations of  $Fe(II)$  correlated strongly with both total fine root biomass and dead fine root biomass at the site scale ( $r = 0.96$  and  $0.94$ , respectively;  $p < 0.01$ ), and showed a negative correlation with crystalline Fe ( $Fe_{cd-ca}$ ). Total fine root biomass also correlated positively with  $Al_{ca}$  ( $r = 0.96$ ,  $p < 0.01$ ), and negatively with bulk density ( $r = -0.97$ ,  $p < 0.01$ ). Pearson correlations between site mean values of all biogeochemical variables and their statistical significance are reported in Supplemental Table 1.

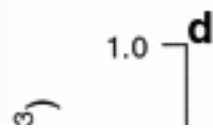
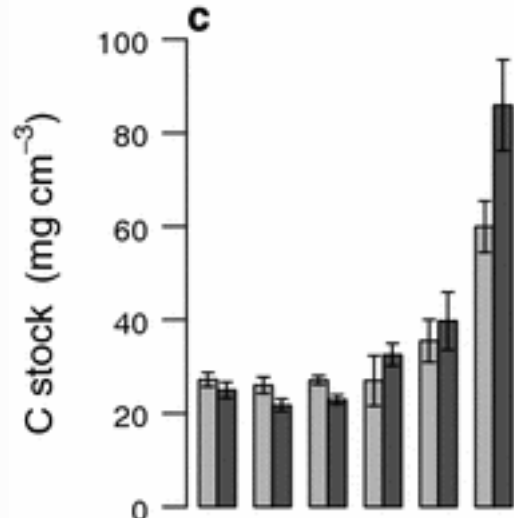
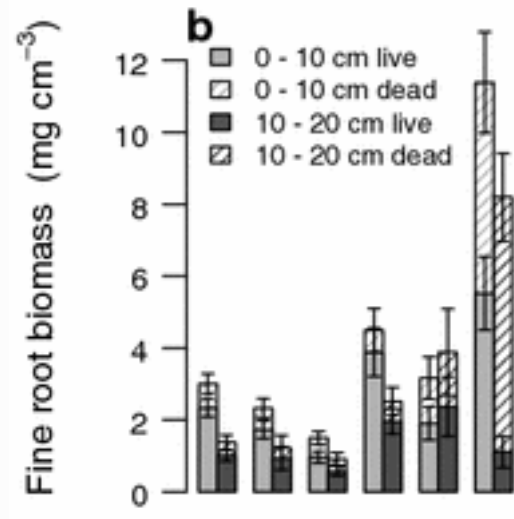
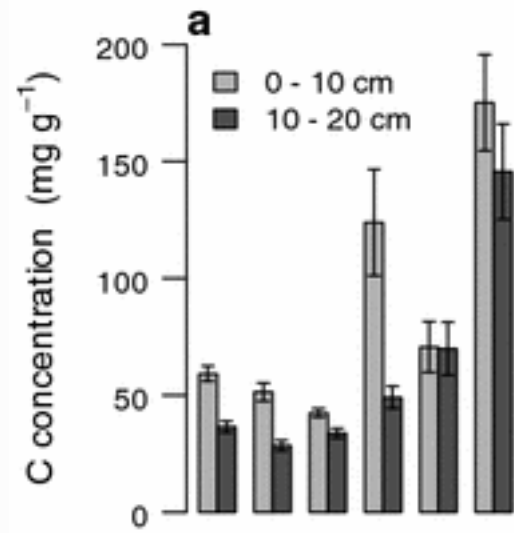


### Fig. 1

Means (SE) of soil attributes by depth increment across the site gradient; mean bulk soil O<sub>2</sub> concentrations decreased by site from *left* to *right*. For the ridge, slope, and valley sites, n = 20 for each *bar*, and for the palm, palo colorado, and elfin sites, n = 5 per *bar*

Surface soil (0–10 cm) C concentrations were greatest in the palm and elfin forests, intermediate in the palo colorado forest, and lowest in the lower montane forest soils, where C concentrations decreased significantly from ridges to slopes to valleys (Fig. 1a; Supplemental Table 2). Shallow subsurface (10–20 cm) C concentrations were significantly greater in the palm, palo colorado, and elfin forests than in the lower montane forest sites, which did not significantly differ from each other (Fig. 1a). In contrast to C concentrations, C stocks in the 0–10 cm increment were similar among all sites with the exception of the elfin forest. In the 10–20 cm soils, C content increased as O<sub>2</sub> declined with elevation across the site gradient (i.e., from left to right in Fig. 1c). Differing trends in C concentrations and stocks among sites were influenced by variation in bulk density, which differed by a factor of three at the site scale and was greatest in the lower montane valleys and lowest in the palm forest (Fig. 1). Patterns in 0–10 cm bulk density corresponded strongly with variation in fine root biomass among sites (Fig. 1b, d). Bulk density in the 10–20 cm depth was less variable and did not differ significantly among sites. Live fine root biomass was greatest in the palm and elfin forests and significantly declined by a factor of two from ridges to valleys in 0–10 cm soil (Fig. 1b). Live fine roots exceeded dead fine root biomass in all sites except for the elfin forest, where dead fine root biomass was more than four-fold greater than the other sites (Fig. 1b).

Soil Fe pools differed greatly among sites (Fig. 2; Table 3). Concentrations of HCl-extractable Fe(II) increased by more than five-fold between the lower montane and elfin sites, whereas the palm and palo colorado sites had intermediate and highly variable Fe(II) concentrations (Fig. 2a). Trends in the Fe(II)/Fe<sub>HCl</sub> ratio across sites were similar to those of Fe(II), with fewer significant differences among sites (Supplemental Table 2). In the lower montane forest soils, Fe(II) concentrations were greatest and equivalent in ridge 0–10 cm and valley 10–20 cm soils over three different sampling events (excluding eight outliers of the 90 total samples with Fe(II) >1000 µg g<sup>-1</sup>), while concentrations were significantly lower in slope soil at the 10–20 cm depth (Supplemental Fig. 1). Crystalline Fe (Fe<sub>cd-ca</sub>) decreased more than two-fold from lower montane slopes to ridges to valleys, which were similar to the palm and palo colorado sites; Fe<sub>cd-ca</sub> was essentially absent in the elfin site (Fig. 2b). Citrate/ascorbate extractable Fe (Fe<sub>ca</sub>) concentrations were greatest in the lower montane ridges and lowest in the palo colorado site (Fig. 2b). Oxalate-extractable Fe (Fe<sub>ox</sub>) concentrations and Fe<sub>ca</sub> were similar in the palm and elfin forests, but Fe<sub>ox</sub> was 30–60 % lower



than  $\text{Fe}_{\text{ca}}$  in the other sites (Fig. 2c). The ratio of  $\text{Fe}_{\text{ca}}/\text{Fe}_{\text{ox}}$  declined significantly and consistently with decreasing  $\text{O}_2$  across all sites (Fig. 2d).

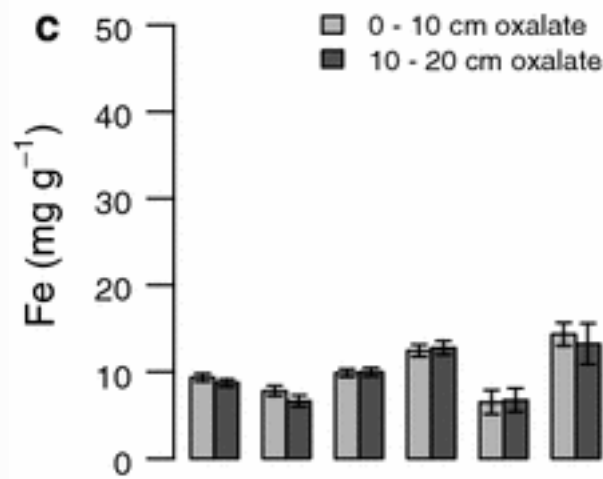
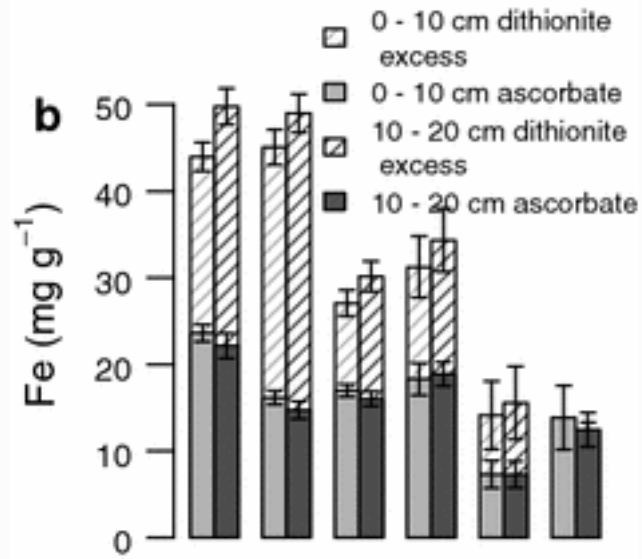
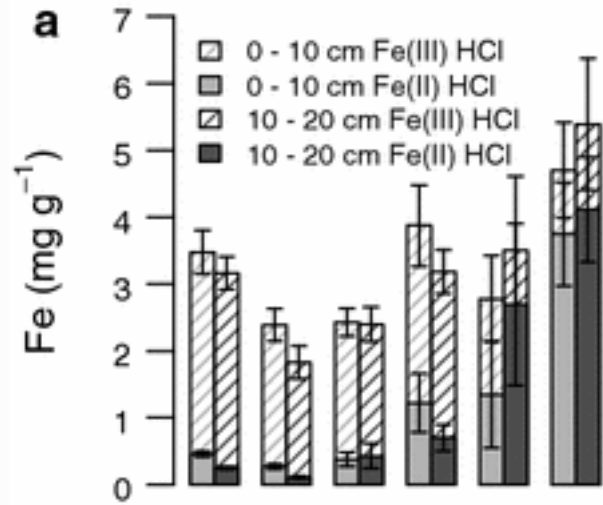


**Fig. 2**

Means (SE) of soil attributes by depth increment across the site gradient; mean bulk soil O<sub>2</sub> concentrations decreased by site

from *left to right*. **a** Concentrations of Fe(II) and Fe(III) in 0.5 M HCl extractions. **b** Fe citrate/ascorbate extractions (Fe<sub>ca</sub>) and citrate/dithionite extractions (Fe<sub>cd</sub>), where the total *bar* height represents Fe<sub>cd</sub>.

The *hashed* portion represents excess Fe in dithionite extractions relative to citrate/ascorbate (Fe<sub>cd-ca</sub>; the difference between citrate/dithionite and citrate/ascorbate extractions), which we interpreted as crystalline Fe. **c** Fe in ammonium oxalate extractions (Fe<sub>ox</sub>). **d** ratios of Fe in citrate/ascorbate to ammonium oxalate. For the ridge, slope, and valley sites, n = 20 for each *bar*, and for the palm, palo colorado, and elfin sites, n = 5 for each *bar*

**Table 3**

Soil attributes by site and depth increment

| Site          | Depth (cm) | Bulk density (g cm <sup>-3</sup> ) | Soil C (mg g <sup>-1</sup> ) | Soil C (mg cm <sup>-3</sup> ) | Live fine roots (mg cm <sup>-3</sup> ) | Total fine roots (mg cm <sup>-3</sup> ) | Sand (%) |
|---------------|------------|------------------------------------|------------------------------|-------------------------------|--|---|----------|
| Ridge         | 0-10       | 0.47 (0.02)                        | 59 (3)                       | 27 (2)                        | 2.3 (0.2)                              | 3 (0.3)                                 | 8 (3)    |
|               | 10-20      | 0.7 (0.04)                         | 37 (2)                       | 25 (2)                        | 1 (0.2)                                | 1.4 (0.2)                               | 7 (0)    |
| Slope         | 0-10       | 0.54 (0.04)                        | 51 (4)                       | 26 (2)                        | 1.7 (0.3)                              | 2.3 (0.3)                               | 10 (1)   |
|               | 10-20      | 0.79 (0.03)                        | 28 (2)                       | 22 (1)                        | 0.9 (0.3)                              | 1.2 (0.3)                               | 12 (1)   |
| Valley        | 0-10       | 0.65 (0.02)                        | 42 (2)                       | 27 (1)                        | 1 (0.2)                                | 1.5 (0.2)                               | 23 (2)   |
|               | 10-20      | 0.7 (0.03)                         | 34 (2)                       | 23 (1)                        | 0.6 (0.1)                              | 0.9 (0.2)                               | 23 (2)   |
| Palm          | 0-10       | 0.24 (0.05)                        | 124 (23)                     | 27 (5)                        | 3.9 (0.7)                              | 4.5 (0.6)                               | 10 (3)   |
|               | 10-20      | 0.68 (0.06)                        | 49 (5)                       | 33 (2)                        | 2 (0.4)                                | 2.5 (0.4)                               | 12 (1)   |
| Palo colorado | 0-10       | 0.51 (0.04)                        | 71 (11)                      | 36 (5)                        | 1.9 (0.5)                              | 3.2 (0.6)                               | 56 (5)   |
|               | 10-20      | 0.6                                | 70 (11)                      | 40 (6)                        | 2.4 (0.8)                              | 3.9 (1.2)                               | 56       |

| Site          | Depth (cm) | Bulk density (g cm <sup>-3</sup> )           | Soil C (mg g <sup>-1</sup> )                | Soil C (mg cm <sup>-3</sup> )          | Live fine roots (mg cm <sup>-3</sup> )    | Total fine roots (mg cm <sup>-3</sup> ) | Sand (%)                               |
|---------------|------------|--|---|--|---|---|--|
|               |            | (0.08)                                       |   |  |   |   | (3)                                    |
| Elfin         | 0-10       | 0.35 (0.01)                                  | 175 (21)                                    | 60 (5)                                 | 5.5 (1)                                   | 11.4 (1.4)                              | 22 (1)                                 |
|               | 10-20      | 0.6 (0.03)                                   | 146 (20)                                    | 86 (10)                                | 1.1 (0.4)                                 | 8.2 (1.2)                               | 22 (1)                                 |
| Site          | Depth (cm) | Fe(III) <sub>HCl</sub> (mg g <sup>-1</sup> ) | Fe(II) <sub>HCl</sub> (mg g <sup>-1</sup> ) | Fe <sub>cd</sub> (mg g <sup>-1</sup> ) | Fe <sub>cd-ca</sub> (mg g <sup>-1</sup> ) | Fe <sub>ca</sub> (mg g <sup>-1</sup> )  | Fe <sub>ox</sub> (mg g <sup>-1</sup> ) |
| Ridge         | 0-10       | 3.5 (0.3)                                    | 0.46 (0.04)                                 | 44 (1.7)                               | 20.4 (2)                                  | 23.6 (1)                                | 9.4 (0.5)                              |
|               | 10-20      | 3.2 (0.2)                                    | 0.25 (0.02)                                 | 49.8 (2.1)                             | 27.6 (2.9)                                | 22.2 (1.5)                              | 8.7 (0.4)                              |
| Slope         | 0-10       | 2.4 (0.2)                                    | 0.27 (0.04)                                 | 45 (2)                                 | 28.9 (2)                                  | 16.2 (0.8)                              | 7.8 (0.6)                              |
|               | 10-20      | 1.8 (0.2)                                    | 0.11 (0.02)                                 | 49 (2.2)                               | 34.2 (2.7)                                | 14.8 (1)                                | 6.6 (0.7)                              |
| Valley        | 0-10       | 2.4 (0.2)                                    | 0.38 (0.11)                                 | 27.1 (1.5)                             | 10.1 (1.3)                                | 17 (0.7)                                | 9.9 (0.5)                              |
|               | 10-20      | 2.4 (0.3)                                    | 0.43 (0.19)                                 | 30.2 (1.7)                             | 14.1 (1.7)                                | 16 (0.9)                                | 10 (0.5)                               |
| Palm          | 0-10       | 3.9 (0.6)                                    | 1.22 (0.44)                                 | 31.2 (3.6)                             | 12.9 (3.2)                                | 18.3 (1.9)                              | 12.5 (0.7)                             |
|               | 10-20      | 3.2 (0.3)                                    | 0.7 (0.2)                                   | 34.3 (3.6)                             | 15.5 (2.9)                                | 18.9 (1.4)                              | 12.8 (0.8)                             |
| Palo Colorado | 0-10       | 2.8 (0.6)                                    | 1.35 (0.8)                                  | 14.2 (3.9)                             | 6.8 (2.5)                                 | 7.3 (1.6)                               | 6.5 (1.4)                              |
|               | 10-20      | 3.5 (1.1)                                    | 2.69 (1.21)                                 | 15.6 (4.2)                             | 8.3 (2.9)                                 | 7.3 (1.5)                               | 6.8 (1.4)                              |

| Site  | Depth (cm) | Fe(III) <sub>HCl</sub> (mg g <sup>-1</sup> ) | Fe(II) <sub>HCl</sub> (mg g <sup>-1</sup> ) | Fe <sub>cd</sub> (mg g <sup>-1</sup> ) | Fe <sub>cd-ca</sub> (mg g <sup>-1</sup> ) | Fe <sub>ca</sub> (mg g <sup>-1</sup> ) | Fe <sub>ox</sub> (mg g <sup>-1</sup> ) |
|-------|------------|--|---|--|---|--|--|
| Elfin | 0–10       | 4.7 (0.7)                                    | 3.74 (0.77)                                 | 11 (0.8)                               | 1.1 (0.6)                                 | 13.9 (3.7)                             | 14.3 (1.4)                             |
|       | 10–20      | 5.4 (1)                                      | 4.11 (0.79)                                 | 11 (2.4)                               | 0.3 (0.3)                                 | 12.5 (2)                               | 13.3 (2.3)                             |

Values represent means and standard errors; n = 20 for each depth increment in the ridge, slope, and valley sites, and n = 5 for the palm, palo colorado, and cloud sites. See Table 2 for abbreviations and “[Soil sampling and analysis](#)” section for details of soil analyses. Citrate/ascorbate and HCl extractions were conducted on moist soils in the field, and the other extractions were conducted on air-dried and ground soils

#### Pairwise relationships between biogeochemical variables and soil C

We assessed pairwise relationships between all measured biogeochemical variables and C concentrations and stocks at the scale of individual samples (n = 149) as a heuristic evaluation prior to reporting mixed-effects models with multiple explanatory variables later in the text, which included random effects to account for spatial autocorrelation at the scale of plots and sites. We found significant positive linear relationships between C concentrations and Al<sub>ca</sub>, Al<sub>ox</sub>, Al<sub>HCl</sub>, Fe(II)<sub>HCl</sub>/Fe<sub>HCl</sub>, Fe<sub>ox</sub>, silt, and fine roots (Fig. 3; R<sup>2</sup> values are reported in the legend). In contrast, we observed negative relationships between C concentrations and Fe<sub>cd-ca</sub> and clay. We found similar overall trends between C stocks and predictor variables, although the strength of pairwise relationships frequently differed (Supplemental Fig. 2; R<sup>2</sup> values are reported in the legend). Carbon stocks increased significantly with Al<sub>ca</sub>, Al<sub>ox</sub>, Al<sub>HCl</sub>, Fe(II)<sub>HCl</sub>/Fe<sub>HCl</sub>, Fe<sub>ox</sub>, silt, sand, and fine roots. Carbon stocks decreased with Fe<sub>cd-ca</sub> and clay. The weak but significant trends between C concentrations and stocks and texture variables (sand, silt, and clay) were driven by extreme values in the montane forest samples (n = 30), as the lower montane samples (n = 119) displayed no significant pairwise relationships with any texture variable when analyzed alone.

[Open image in new window](#)

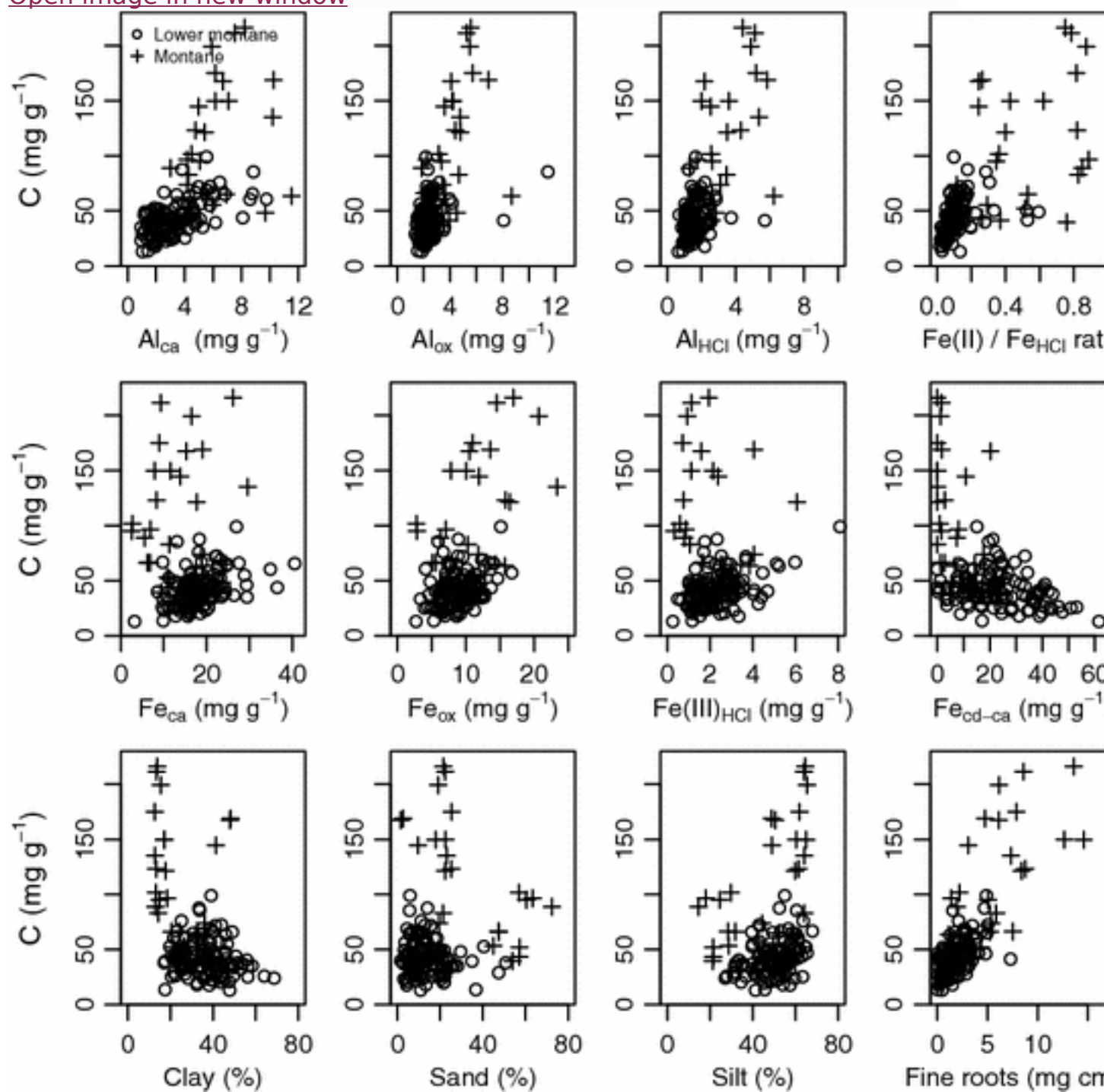


**Fig. 3**

Pairwise relationships between soil C concentrations and biogeochemical variables described in Table 2. Total  $n = 149$  for each scatterplot, with 119 samples from the lower montane and 30 from the montane sites; two outliers with Fe(II) concentrations  $>10 \text{ mg g}^{-1}$  are not shown. As a heuristic, we report  $R^2$  and statistical significance for each scatterplot, acknowledging an overestimate of  $R^2$  due to the spatial structure of our data:  $\text{Al}_{\text{ca}}$  ( $R^2 = 0.35$ ,

$p < 0.0001$ );  $Al_{ox}$  ( $R^2 = 0.29$ ,  $p < 0.0001$ );  $Al_{HCl}$  ( $R^2 = 0.31$ ,  $p < 0.0001$ );  $Fe(II)_{HCl}/Fe_{HCl}$  ( $R^2 = 0.47$ ,  $p < 0.0001$ );  $Fe_{ca}$  ( $R^2 = 0.01$ ,  $p = 0.29$ );  $Fe_{ox}$  ( $R^2 = 0.18$ ,  $p < 0.0001$ );  $Fe(III)_{HCl}$  ( $R^2 = 0.01$ ;  $p = 0.86$ );  $Fe_{cd-ca}$  ( $R^2 = 0.22$ ,  $p < 0.0001$ ); clay ( $R^2 = 0.14$ ,  $p < 0.0001$ ); sand ( $R^2 = 0.10$ ,  $p = 0.10$ ); silt ( $R^2 = 0.07$ ,  $p < 0.001$ ); total fine roots ( $R^2 = 0.61$ ,  $p < 0.0001$ )

## Statistical models for predicting soil C concentrations and stocks

The optimal mixed-effects model for C concentrations in individual soil samples from the lower montane forest ( $n = 119$ ) showed that C significantly increased with total fine root biomass,  $Al_{ca}$ ,  $Fe_{ox}$ , an index of reducing conditions ( $Fe(II)/Fe_{HCl}$ ),  $Fe(III)_{HCl}$ , and an interaction between  $Fe(II)/Fe_{HCl}$  and  $Al_{ca}$ , while C concentrations significantly decreased with depth and  $Fe_{ca}$  (Supplemental Table 3). The overall model pseudo  $R^2$  was 0.72, and seven of the eight predictor variables were significant at  $p < 0.001$ , whereas the remaining variable ( $Fe(II)/Fe_{HCl} \times Al_{ca}$  interaction) was significant at  $p < 0.01$ . The optimum model of soil C concentrations for the entire dataset ( $n = 149$ ) was quite similar to the model for the lower montane samples alone, although it did not include  $Fe_{HCl}$ , and the pseudo  $R^2$  value was 0.82.

The optimum model of individual sample soil C stocks for the lower montane soils was broadly consistent with the model of C concentrations, although it contained fewer fixed effects and had much lower explanatory power (pseudo  $R^2 = 0.18$ ; Supplemental Table 4). The model showed that C stocks increased with  $Fe_{ox}$  and  $Al_{ca}$ , and decreased with  $Fe_{ca}$  and depth. The model of C stocks for the overall dataset, in contrast, included more predictor variables and had greater explanatory power (pseudo  $R^2 = 0.60$ ). Overall, C stocks increased with  $Fe(II)/Fe_{HCl}$ ,  $Fe_{ox}$ ,  $Al_{ca}$ , an interaction between  $Fe(II)/Fe_{HCl}$  and  $Al_{ca}$ , and decreased with  $Fe_{ca}$ . This model did not include an effect of soil depth, indicating that the other predictor variables captured the effect of depth on soil C stocks.

## Discussion

Biogeochemical predictors including reducing conditions, multiple pools of reactive Al and Fe, and fine root biomass could explain a large majority of the spatial variation in surface soil C in sites spanning a broad range of biophysical environments in the Luquillo Experimental Forest. Given the observational nature of this study, we cannot interpret our findings in terms of causation, but we suggest that the patterns observed here reflect underlying biogeochemical mechanisms. Site mean C concentrations and stocks ( $n = 6$ ) were very strongly related to an index of reducing conditions and root biomass, whereas the mixed-effects models of individual C samples implied the additional importance of several indices of reactive Al and Fe at finer spatial scales. These were indicated by highly significant model coefficients, overall high explanatory power, and a decreased importance of



root biomass in the sample-scale mixed-effects model. In contrast, the low  $R^2$  values of univariate pairwise comparisons between C and predictor variables at the scale of individual soil samples indicated the importance of additive and interactive relationships between biogeochemical drivers and soil C concentrations and stocks. It is unsurprising that the mixed-effects models of soil C at the scale of individual samples included additional biogeochemical variables not evident at the coarser scale of sites, as these models had much greater spatial resolution and statistical power to detect relationships between soil C and potential predictors. Additionally, the sample-scale models allowed us to assess the importance of biogeochemical spatial heterogeneity within sites as well as among sites, which was important for teasing apart relationships between soil C and multiple indices of reactive Fe and Al.

Variation in total C among samples was likely driven by changes in both mineral-associated and particulate C. Previous studies have shown a predominance (75–90 %, mass basis) of mineral-associated C relative to particulate C across the lower montane tabonuco and palo colorado forests, including the same sites examined here (Cusack et al. [2011](#); Hall et al. [2015a](#)). Soil C concentrations and stocks often showed distinct patterns among sites due to co-variation in bulk density, as reported by previous studies in the Luquillo Experimental Forest (Johnson et al. [2015](#)). Variation in bulk density was likely driven predominantly by variation in fine root biomass and consequent impacts on soil aggregation, given the very strong negative correlation between fine roots and bulk density across all sites. In contrast, light fraction C content likely had less impact on variation in bulk density. Light fraction C varied little among topographic positions in the lower montane forest despite high variation in bulk density, and represented a consistently minor portion (13 %) of total soil C (Hall et al. [2015a, b](#)). The sierra palm and elfin forests likely had a greater proportion of particulate C, as suggested by large increases in total soil C concentrations. McGroddy and Silver ([2000](#)) found that particulate C comprised approximately 70 % of total soil C in a sparsely forested site at an even higher elevation than the elfin forest examined here, providing a likely upper bound on the contribution of particulate C in the present study. Another recent study in the Luquillo Experimental Forest found that soil C content strongly increased with soil C/N ratios (Johnson et al. [2015](#)). This pattern could reflect the effects of increasing particulate C abundance, given that particulate C has a greater C/N ratio than mineral-associated C (Cusack et al. [2011](#)). Despite likely differences in the proportion of mineral-associated versus particulate C among sites, it is notable that predictors of total soil C in mixed-effects models were highly similar when comparing the lower montane sites alone (which had very little particulate C) with the entire dataset.

We have no data describing soil organic matter turnover rates in the montane sites examined here, but mineral-associated C turnover was well constrained in the lower montane forest using radiocarbon measurements and modeling in a separate study. The majority (66 %) of mineral-associated C sampled across a topographic catena turned over rapidly (11–26 year) (Hall et al. [2015a, b](#)). In that study, increasing Fe(II) concentrations were associated with longer turnover times of mineral-associated C, and were the only variable significantly related to turnover rates. In the lower montane forest, we expect that variation in C concentrations was primarily driven by mineral-associated C abundance, given that the relatively small pool of particulate C in these sites ( $13 \pm 2$  % of total C; Hall et al. [2015a, b](#)) would not be large enough to explain the high variability in total C concentrations among samples. However, in the montane forest it is likely that strongly reducing conditions and high root biomass allocation contributed to particulate C accumulation, possibly analogous to a mineral-rich peatland soil (Fenner and Freeman [2011](#)).

## Relationships between litterfall, fine root biomass, and soil C content

Spatial patterns in soil C among sites appeared to primarily reflect variation in factors controlling soil organic matter decomposition rates as opposed to C inputs. Soil C concentrations and stocks increased with site-level indices of reducing conditions even as litterfall, a proxy for NPP, decreased. A similar pattern of decreasing aboveground C inputs and increasing soil C was observed across an elevation gradient of Hawaiian tropical montane forests (Schuur et al. [2001](#)). However, relationships between soil C and root biomass were more difficult to interpret. Given that litterfall declined at the site scale as root biomass increased, the strong and highly significant pairwise relationships observed between fine root biomass and soil C at the site scale were unlikely to reflect increased C inputs from higher root productivity. Rather, the accumulation of high root standing stocks (dominated by dead biomass at the montane sites) may simply reflect low rates of particulate organic matter decomposition under reducing conditions, leading to an increased particulate fraction of soil C. Increased root biomass could also reflect plant nutrient limitation and long-term investment in root biomass to promote nutrient acquisition, but not necessarily reflect increased root productivity (Vogt et al. [1996](#); Ostertag [2001](#); Espeleta and Clark [2007](#)). Regardless of the degree to which fine root biomass stocks may reflect C inputs versus rates of C losses, fine root biomass provided an exceptionally strong proxy for surface soil C concentrations at the site scale, but was much less important in mixed-effects models of soil C at the scale of individual samples after other covariates were accounted for.

## Reducing conditions and C accumulation

We observed very strong relationships between an index of reducing conditions (Fe(II) concentrations) and soil C at the scale of sites and individual samples, indicative of the overall importance of anaerobiosis in retarding decomposition. Recent studies have also showed the importance of periodic anaerobiosis in promoting C mobilization and degradation (Thompson et al. [2006](#); Hall and Silver [2013](#); Hall et al. [2014](#); Buettner et al. [2014](#); Hall et al. [2015b](#)), although our present data suggest that inhibitory effects of anaerobiosis on organic matter decomposition may predominate at the landscape scale. The Fe(II) concentrations that we measured, especially in the montane palm, palo colorado, and elfin forest sites, were similar to those measured in flooded wetland sediments and rice paddy soils under anaerobic conditions (Roden and Wetzel [1996](#); Frenzel et al. [1999](#)). In the upland, non-flooded soils examined here, high Fe(II) concentrations and differences between soil O<sub>2</sub> and Fe(II) among sites likely reflect the prevalence of reducing conditions in microsites within a porous soil matrix, which typically contains substantial gas-phase O<sub>2</sub> (Silver et al. [1999](#)).

## Multiple relationships between Fe pools and soil C

Crystalline Fe oxides (Fe<sub>cd-ca</sub>) declined precipitously with mean soil O<sub>2</sub> across sites at the landscape scale, presumably reflecting weathering over pedogenic timescales, whereas Fe<sub>ox</sub> varied relatively little. Thompson et al. ([2011](#)) observed a similar pattern across a Hawaiian gradient of basaltic soils, where increased precipitation depleted Fe oxyhydroxides while organic and silicate-bound Fe were retained. The ratio of Fe<sub>ca</sub> to Fe<sub>ox</sub> also showed a consistent decline with mean soil O<sub>2</sub> across sites. We hypothesize that this pattern might reflect the progressive depletion of excess Fe<sub>ca</sub> relative to Fe<sub>ox</sub> by reductive dissolution and leaching, along with the relative retention of Fe co-precipitated with organic matter and/or Al, which could be less vulnerable to reductive dissolution. Supporting this idea, Varela and Tien ([2003](#)) demonstrated that high concentrations of organic ligands can inhibit Fe reduction. Whereas Fe<sub>ox</sub> represented a dominant Fe fraction in the sites with greatest soil C concentrations and lowest O<sub>2</sub>, crystalline Fe (Fe<sub>cd-ca</sub>) was negligible. The lack of a relationship between crystalline Fe and C is unsurprising given that it has relatively less reactive surface area than short range-order Fe phases likely represented by Fe<sub>ox</sub>.

Co-variation in Fe<sub>ca</sub>/Fe<sub>ox</sub> and C at the site scale may help explain opposing relationships between soil C concentrations and these two Fe pools in the mixed-effects models of individual soil samples. Mixed-effects models allowed us to test relationships between soil C and multiple co-varying predictor variables while including random effects to account for spatial correlation. Positive relationships between Fe<sub>ox</sub> and soil C are consistent with a wide body of work reflecting the importance of Fe-C sorption and co-precipitation in protecting C from microbial decomposition (e.g. Kaiser and

Guggenberger [2000](#); Powers and Schlesinger [2002](#); Kleber et al. [2005](#)). More interesting, however, was the highly significant negative relationship between C concentrations and  $Fe_{ca}$ , which was consistent regardless of whether  $Fe_{ox}$  was included in the mixed-effects models or not. We hypothesize that this relationship reflects the importance of Fe reduction as a mechanism of C loss. In other words, the availability of excess reducible, short-range order Fe oxides to catalyze anaerobic microbial respiration in humid tropical ecosystems may partially offset soil C accumulation under reducing conditions, despite the fact that organo-Fe interactions are also demonstrably associated with C accumulation. Dissimilatory Fe reduction is the dominant anaerobic respiratory process in these soils and accounts for a significant portion of ecosystem metabolism (Dubinsky et al. [2010](#)), and anaerobic decomposition has been shown to increase with the availability of reactive Fe oxides (Sutton-Grier et al. [2011](#)). Short-term respiration rates are similar under aerobic and anaerobic conditions in soils from lower montane forest ridges (McNicol and Silver [2014](#)), exemplifying the importance of Fe reduction in sustaining high rates of decomposition. These multiple biogeochemical functions of reactive Fe could help explain multiple relationships—positive, negative, and neutral—previously reported between Fe measured in different soil extractions and C concentrations in humid tropical ecosystems (Powers and Schlesinger [2002](#); Koning et al. [2003](#); Powers and Veldkamp [2005](#); Tonnejck et al. [2010](#)). Further work is needed to assess the multiple potential roles of Fe in soil C cycling, especially the characterization of pools isolated by extractions and their spatial relationship with organic matter.

## Relationships between extractable Al and soil C

Concentrations of  $Al_{ca}$  were the strongest individual correlate of sample-scale C concentrations in mixed-effects models. While the precise speciation of  $Al_{ca}$  is uncertain, it likely includes a substantial portion of organically-complexed Al as well as Al co-precipitated with short-range order Fe oxides. The positive relationship between  $Al_{ca}$  and C concentrations and stocks suggests the importance of organo-Al complexation, cation bridging, and possibly C sorption to short-range ordered Al minerals in contributing to C stabilization in soils across the landscape. Similar patterns are apparent across a wide range of soil types, although they have predominantly been demonstrated in Andisols (Torn et al. [1997](#); Percival et al. [2000](#); Powers and Schlesinger [2002](#); Kleber et al. [2005](#); Wagai and Mayer [2007](#); Tonnejck et al. [2010](#)). Meanwhile, clay content showed no relationship with soil C concentrations or stocks, similar to the findings of Percival et al. ([2000](#)). The absence of a relationship between soil C and clay content is unsurprising in these soils given that they are dominated by kaolinite (Peretyazhko and Sposito [2005](#)), which is less reactive than the 2:1 phyllosilicate clays.

One implication of the mixed-effects models is that reducing conditions and the co-precipitation or sorption of organic compounds by reactive Al appear to have additive impacts on organic matter accumulation, or possibly promote the accumulation of different forms of C (particulate vs. mineral-associated). In addition, the mixed-effects models suggested a strong interactive relationship between  $Al_{ca}$  and reducing conditions, where simultaneous increases in concentrations of  $Al_{ca}$  and Fe(II) were associated with greater C than expected from either variable alone. This relationship may simply indicate the importance of some other unmeasured covariate that led to C accumulation in samples that were especially rich in  $Al_{ca}$  and Fe(II), or it could be indicative of an underlying mechanism. For example, the positive interaction between  $Al_{ca}$  and reducing conditions with soil C concentrations might also imply the importance of molecular  $O_2$  as a co-reactant to decompose organic matter associated with Al, given that oxidase enzymes and reactive oxygen species are well known to be potent agents of organic matter solubilization (Sinsabaugh [2010](#)) that could disrupt metal/organic complexes.

## Conclusions

In current conceptual frameworks of soil C cycling in upland ecosystems, sorption and complexation of organic matter by reactive metals and minerals are thought to strongly influence spatial patterns of soil C accumulation, whereas the availability and influence of  $O_2$  and other oxidants (e.g. Fe oxides) on decomposition have received less attention. Previous studies of soil C in humid tropical forests often focused on relationships between C and soil mineralogy and geochemistry. We found that a relatively small suite of variables, including a proxy for reducing conditions, multiple indices of reactive Fe and Al, and fine root biomass could explain a majority of the variation in C concentrations and stocks across a humid tropical forest landscape. Co-variation among fine root biomass, reducing conditions, and soil C likely reflected impacts of reducing conditions on organic matter decomposition rates. Mixed-effects models also suggested the importance of a positive interaction between reducing conditions and Al-organic complexation in promoting C accumulation. We found, however, that C concentrations declined with the availability of reducible Fe (citrate/ascorbate extraction) that can sustain anaerobic microbial respiration, independent of the positive relationships between C and reducing conditions and  $Fe_{ox}$ . Our findings imply the importance of nuanced and multifaceted relationships between reducing conditions, roots, and reactive metals/minerals in understanding the distribution of soil organic matter in humid tropical forests, which represent exceptionally productive ecosystems with important links to the global climate system.

## Notes

## Acknowledgments

All data reported here will be publicly available through the NSF Critical Zone Observatory web data repository (<http://criticalzone.org/luquillo/data/>). We thank T. Baisden, M. Kramer, and anonymous reviewers for critical commentary. G. Sposito, A. Thompson, M. Firestone, and R. Rhew also provided valuable insights, and H. Dang, J. Treffkorn, T. Natake, J. Cosgrove, R. Ryals, A. McDowell, and C. Torrens helped in the field and lab. SJH was funded by the DOE Office of Science Graduate Fellowship Program supported by the American Recovery and Reinvestment Act of 2009, administered by ORISE-ORAU under contract no. DE-AC05-06OR23100. WLS received support from CA-B-ECO-7673-MS from the A.E.S. Funding was also provided by DOE grant DE-FOA-0000749 and NSF grant EAR-08199072 to WLS, the NSF Luquillo Critical Zone Observatory (EAR-0722476) with additional support provided by the USGS Luquillo WEBB program, and grant DEB 0620910 from NSF to the Institute for Tropical Ecosystem Studies, University of Puerto Rico, and to the International Institute of Tropical Forestry USDA Forest Service, as part of the LTER Program.

## Supplementary material

[10533\\_2015\\_120\\_MOESM1\\_ESM.docx](#) (1.3 mb)

Supplementary material 1 (DOCX 1375 kb)

## References

1. Baldock JA, Skjemstad JO (2000) Role of the soil matrix and minerals in protecting natural organic materials against biological attack. *Org Geochem* 31:697-710. doi: [10.1016/S0146-6380\(00\)00049-8](https://doi.org/10.1016/S0146-6380(00)00049-8)[CrossRefGoogle Scholar](#)
2. Bruun TB, Elberling B, Christensen BT (2010) Lability of soil organic carbon in tropical soils with different clay minerals. *Soil Biol Biochem* 42:888-895. doi: [10.1016/j.soilbio.2010.01.009](https://doi.org/10.1016/j.soilbio.2010.01.009)[CrossRefGoogle Scholar](#)
3. Buettner SW, Kramer MG, Chadwick OA, Thompson A (2014) Mobilization of colloidal carbon during iron reduction in basaltic soils. *Geoderma* 221-222:139-145. doi: [10.1016/j.geoderma.2014.01.012](https://doi.org/10.1016/j.geoderma.2014.01.012)[CrossRefGoogle Scholar](#)
4. Chinea JD, Beymer RJ, Rivera C, Sastre de Jesus I, Scatena FN (1994) An annotated list of flora of the Bisley area, Luquillo Experimental Forest, Puerto Rico. US Department of Agriculture, Forest Service, General Technical Report SO-94, New Orleans[Google Scholar](#)
5. Christensen TH, Bjerg PL, Banwart SA et al (2000) Characterization of redox conditions in groundwater contaminant plumes. *J Contam Hydrol*



45:165–241. doi: [10.1016/S0169-7722\(00\)00109-1](https://doi.org/10.1016/S0169-7722(00)00109-1)[CrossRefGoogle Scholar](#)

6. Cleveland CC, Wieder WR, Reed SC, Townsend AR (2010) Experimental drought in a tropical rain forest increases soil carbon dioxide losses to the atmosphere. *Ecology* 91:2313–2323. doi: [10.1890/09-1582.1](https://doi.org/10.1890/09-1582.1)[CrossRefGoogle Scholar](#)
7. Cusack DF, Chou WW, Yang WH et al (2009) Controls on long-term root and leaf litter decomposition in neotropical forests. *Glob Change Biol* 15:1339–1355. doi: [10.1111/j.1365-2486.2008.01781.x](https://doi.org/10.1111/j.1365-2486.2008.01781.x)[CrossRefGoogle Scholar](#)
8. Cusack DF, Silver WL, Torn MS, McDowell WH (2011) Effects of nitrogen additions on above- and belowground carbon dynamics in two tropical forests. *Biogeochemistry* 104:203–225. doi: [10.1007/s10533-010-9496-4](https://doi.org/10.1007/s10533-010-9496-4)[CrossRefGoogle Scholar](#)
9. de Koning GHJ, Veldkamp E, López-Ulloa M (2003) Quantification of carbon sequestration in soils following pasture to forest conversion in northwestern Ecuador. *Glob Biogeochem Cycles* 17:1098. doi: [10.1029/2003GB002099](https://doi.org/10.1029/2003GB002099)[CrossRefGoogle Scholar](#)
10. DeAngelis KM, Chivian D, Fortney JL et al (2013) Changes in microbial dynamics during long-term decomposition in tropical forests. *Soil Biol Biochem* 66:60–68. doi: [10.1016/j.soilbio.2013.06.010](https://doi.org/10.1016/j.soilbio.2013.06.010)[CrossRefGoogle Scholar](#)
11. Dieleman WIJ, Venter M, Ramachandra A et al (2013) Soil carbon stocks vary predictably with altitude in tropical forests: implications for soil carbon storage. *Geoderma* 204–205:59–67. doi: [10.1016/j.geoderma.2013.04.005](https://doi.org/10.1016/j.geoderma.2013.04.005)[CrossRefGoogle Scholar](#)
12. Dubinsky EA, Silver WL, Firestone MK (2010) Tropical forest soil microbial communities couple iron and carbon biogeochemistry. *Ecology* 91:2604–2612. doi: [10.1890/09-1365.1](https://doi.org/10.1890/09-1365.1)[CrossRefGoogle Scholar](#)
13. Espeleta JF, Clark DA (2007) Multi-scale variation in fine-root biomass in a tropical rain forest: a seven-year study. *Ecol Monogr* 77:377–404. doi: [10.1890/06-1257.1](https://doi.org/10.1890/06-1257.1)[CrossRefGoogle Scholar](#)
14. Fenner N, Freeman C (2011) Drought-induced carbon loss in peatlands. *Nat Geosci* 4:895–900. doi: [10.1038/NNGEO1323](https://doi.org/10.1038/NNGEO1323)
15. Fredrickson JK, Zachara JM, Kennedy DW et al (1998) Biogenic iron mineralization accompanying the dissimilatory reduction of hydrous ferric oxide by a groundwater bacterium. *Geochim Cosmochim Acta*



62:3239–3257. doi: [10.1016/S0016-7037\(98\)00243-9](https://doi.org/10.1016/S0016-7037(98)00243-9)[CrossRef](#)[Google Scholar](#)

16. Frenzel P, Bosse U, Janssen PH (1999) Rice roots and methanogenesis in a paddy soil: ferric iron as an alternative electron acceptor in the rooted soil. *Soil Biol Biochem* 31:421–430. doi: [10.1016/S0038-0717\(98\)00144-8](https://doi.org/10.1016/S0038-0717(98)00144-8)[CrossRef](#)[Google Scholar](#)
17. Gee G, Bauder J (1986) Particle size analysis. In: Klute A (ed) *Methods of soil analysis, Part 1, physical and mineralogical methods*, 2nd edn. American Society of Agronomy, Madison, pp 383–411[Google Scholar](#)
18. Hall SJ, Silver WL (2013) Iron oxidation stimulates organic matter decomposition in humid tropical forest soils. *Glob Change Biol* 19:2804–2813. doi: [10.1111/gcb.12229](https://doi.org/10.1111/gcb.12229)[CrossRef](#)[Google Scholar](#)
19. Hall SJ, McDowell WH, Silver WL (2013) When wet gets wetter: decoupling of moisture, redox biogeochemistry, and greenhouse gas fluxes in a humid tropical forest soil. *Ecosystems* 16:576–589. doi: [10.1007/s10021-012-9631-2](https://doi.org/10.1007/s10021-012-9631-2)[CrossRef](#)[Google Scholar](#)
20. Hall SJ, Treffkorn J, Silver WL (2014) Breaking the enzymatic latch: impacts of reducing conditions on hydrolytic enzyme activity in tropical forest soils. *Ecology* 95:2964–2973. doi: [10.1890/13-2151.1](https://doi.org/10.1890/13-2151.1)[CrossRef](#)[Google Scholar](#)
21. Hall SJ, McNicol G, Natake T, Silver WL (2015a) Large fluxes and rapid turnover of mineral-associated carbon across topographic gradients in a humid tropical forest: insights from paired <sup>14</sup>C analysis. *Biogeosci Discuss* 12:891–932. doi: [10.5194/bgd-12-891-2015](https://doi.org/10.5194/bgd-12-891-2015)[CrossRef](#)[Google Scholar](#)
22. Hall SJ, Silver WL, Timokhin VI, Hammel KE (2015b) Lignin decomposition is sustained under fluctuating redox conditions in humid tropical forest soils. *Glob Change Biol* 21:2818–2828. doi: [10.1111/gcb.12908](https://doi.org/10.1111/gcb.12908)[CrossRef](#)[Google Scholar](#)
23. Heartsill Scalley T, Scatena FN, Lugo AE et al (2010) Changes in structure, composition, and nutrients during 15 year of hurricane-induced succession in a subtropical wet forest in Puerto Rico. *Biotropica* 42:455–463. doi: [10.1111/j.1744-7429.2009.00609.x](https://doi.org/10.1111/j.1744-7429.2009.00609.x)[CrossRef](#)[Google Scholar](#)
24. Hyacinthe C, Bonneville S, Van Cappellen P (2006) Reactive iron(III) in sediments: chemical versus microbial extractions. *Geochim Cosmochim Acta* 70:4166–4180. doi: [10.1016/j.gca.2006.05.018](https://doi.org/10.1016/j.gca.2006.05.018)[CrossRef](#)[Google Scholar](#)

25. Jobbagy EG, Jackson RB (2000) The vertical distribution of soil organic carbon and its relation to climate and vegetation. *Ecol Appl* 10:423–436. doi: [10.1890/1051-0761\(2000\)010\[0423:TVDOSO\]2.0.CO;2](https://doi.org/10.1890/1051-0761(2000)010[0423:TVDOSO]2.0.CO;2)
26. Johnson AH, Xing HX, Scatena FN (2015) Controls on soil carbon stocks in El Yunque National Forest, Puerto Rico. *Soil Sci Soc Am J* 79:294. doi: [10.2136/sssaj2014.05.0199](https://doi.org/10.2136/sssaj2014.05.0199)[CrossRefGoogle Scholar](#)
27. Kaiser K, Guggenberger G (2000) The role of DOM sorption to mineral surfaces in the preservation of organic matter in soils. *Org Geochem* 31:711–725. doi: [10.1016/S0146-6380\(00\)00046-2](https://doi.org/10.1016/S0146-6380(00)00046-2)[CrossRefGoogle Scholar](#)
28. Kleber M, Mikutta R, Torn MS, Jahn R (2005) Poorly crystalline mineral phases protect organic matter in acid subsoil horizons. *Eur J Soil Sci* 56:717–725. doi: [10.1111/j.1365-2389.2005.00706.x](https://doi.org/10.1111/j.1365-2389.2005.00706.x)[Google Scholar](#)
29. Kramer MG, Sanderman J, Chadwick OA et al (2012) Long-term carbon storage through retention of dissolved aromatic acids by reactive particles in soil. *Glob Change Biol* 18:2594–2605. doi: [10.1111/j.1365-2486.2012.02681.x](https://doi.org/10.1111/j.1365-2486.2012.02681.x)[CrossRefGoogle Scholar](#)
30. Liptzin D, Silver WL, Detto M (2011) Temporal dynamics in soil oxygen and greenhouse gases in two humid tropical forests. *Ecosystems* 14:171–182. doi: [10.1007/s10021-010-9402-x](https://doi.org/10.1007/s10021-010-9402-x)[CrossRefGoogle Scholar](#)
31. Loeppert R, Inskeep W (1996) Iron. In: Sparks D (ed) *Methods of soil analysis, part 3—chemical methods*. Soil Science Society of America, Madison, pp 639–664[Google Scholar](#)
32. Malhi Y, Grace J (2000) Tropical forests and atmospheric carbon dioxide. *Trends Ecol Evol* 15:332–337. doi: [10.1016/S0169-5347\(00\)01906-6](https://doi.org/10.1016/S0169-5347(00)01906-6)[CrossRefGoogle Scholar](#)
33. McDowell WH, Scatena FN, Waide RB et al (2012) Geographic and ecological setting of the Luquillo Mountains. In: Brokaw N, Crowl T, Lugo A et al (eds) *A caribbean forest tapestry: the multidimensional nature of disturbance and response*. Oxford University Press, New York, pp 72–163[CrossRefGoogle Scholar](#)
34. McGroddy M, Silver WL (2000) Variations in belowground carbon storage and soil CO<sub>2</sub> flux rates along a wet tropical climate gradient. *Biotropica* 32:614–624[CrossRefGoogle Scholar](#)
35. McNicol G, Silver WL (2014) Separate effects of flooding and anaerobiosis on soil greenhouse gas emissions and redox sensitive

biogeochemistry. *J Geophys Res Biogeosci.*  
doi: [10.1002/2013JG002433](https://doi.org/10.1002/2013JG002433)[Google Scholar](#)

36. Nakagawa S, Schielzeth H (2013) A general and simple method for obtaining R<sup>2</sup> from generalized linear mixed-effects models. *Method Ecol Evol* 4:133–142. doi: [10.1111/j.2041-210x.2012.00261.x](https://doi.org/10.1111/j.2041-210x.2012.00261.x)[CrossRef](#)[Google Scholar](#)
37. Ostertag R (2001) Effects of nitrogen and phosphorus availability on fine-root dynamics in Hawaiian montane forests. *Ecology* 82:485–499. doi: [10.1890/0012-9658\(2001\)082\[0485:EONAPA\]2.0.CO;2](https://doi.org/10.1890/0012-9658(2001)082[0485:EONAPA]2.0.CO;2)
38. Parton W, Silver WL, Burke IC et al (2007) Global-scale similarities in nitrogen release patterns during long-term decomposition. *Science* 315:361–364. doi: [10.1126/science.1134853](https://doi.org/10.1126/science.1134853)[CrossRef](#)[Google Scholar](#)
39. Percival HJ, Parfitt RL, Scott NA (2000) Factors controlling soil carbon levels in New Zealand grasslands. *Soil Sci Soc Am J* 64:1623. doi: [10.2136/sssaj2000.6451623x](https://doi.org/10.2136/sssaj2000.6451623x)[CrossRef](#)[Google Scholar](#)
40. Peretyazhko T, Sposito G (2005) Iron(III) reduction and phosphorous solubilization in humid tropical forest soils. *Geochim Cosmochim Acta* 69:3643–3652. doi: [10.1016/j.gca.2005.03.045](https://doi.org/10.1016/j.gca.2005.03.045)[CrossRef](#)[Google Scholar](#)
41. Phillips EJP, Lovley DR, Roden EE (1993) Composition of non-microbially reducible Fe(III) in aquatic sediments. *Appl Environ Microbiol* 59:2727–2729[Google Scholar](#)
42. Pinheiro J, Bates D, DebRoy S et al (2014) nlme: linear and nonlinear mixed effects models. R package version 3.1. <http://CRAN.R-project.org/package=nlme>
43. Ponnampetuma FN (1972) The chemistry of submerged soils. *Adv Agron* 24:29–96[CrossRef](#)[Google Scholar](#)
44. Powers JS, Schlesinger WH (2002) Relationships among soil carbon distributions and biophysical factors at nested spatial scales in rain forests of northeastern Costa Rica. *Geoderma* 109:165–190. doi: [10.1016/S0016-7061\(02\)00147-7](https://doi.org/10.1016/S0016-7061(02)00147-7)[CrossRef](#)[Google Scholar](#)
45. Powers JS, Veldkamp E (2005) Regional variation in soil carbon and  $\delta^{13}\text{C}$  in forests and pastures of northeastern Costa Rica. *Biogeochemistry* 72:315–336. doi: [10.1007/s10533-004-0368-7](https://doi.org/10.1007/s10533-004-0368-7)[CrossRef](#)[Google Scholar](#)

46. Rasse DP, Rumpel C, Dignac M-F (2005) Is soil carbon mostly root carbon? Mechanisms for a specific stabilisation. *Plant Soil* 269:341–356. doi: [10.1007/s11104-004-0907-y](https://doi.org/10.1007/s11104-004-0907-y)[CrossRef](#)[Google Scholar](#)
47. Reyes I, Torrent J (1997) Citrate-ascorbate as a highly selective extractant for poorly crystalline iron oxides. *Soil Sci Soc Am J* 61:1647–1654[CrossRef](#)[Google Scholar](#)
48. Roden E, Wetzel R (1996) Organic carbon oxidation and suppression of methane production by microbial Fe(III) oxide reduction in vegetated and unvegetated freshwater wetland sediments. *Limnol Oceanogr* 41:1733–1748[CrossRef](#)[Google Scholar](#)
49. Scatena FN, Lugo AE (1995) Geomorphology, disturbance, and the soil and vegetation of two subtropical wet steepland watersheds of Puerto Rico. *Geomorphology* 13:199–213[Google Scholar](#)
50. Scatena FN, Moya S, Estrada C, China JD (1996) The first five years in the reorganization of aboveground biomass and nutrient use following Hurricane Hugo in the Bisley Experimental Watersheds, Luquillo Experimental Forest, Puerto Rico. *Biotropica* 28:424–440[Google Scholar](#)
51. Schuur EAG (2001) The effect of water on decomposition dynamics in mesic to wet Hawaiian montane forests. *Ecosystems* 4:259–273. doi: [10.1007/s10021-001-0008-1](https://doi.org/10.1007/s10021-001-0008-1)[CrossRef](#)[Google Scholar](#)
52. Schuur EAG, Chadwick OA, Matson PA (2001) Carbon cycling and soil carbon storage in mesic to wet Hawaiian montane forests. *Ecology* 82:3182–3196. doi:10.1890/0012-9658(2001)082[3182:CCASCS]2.0.CO;2[Google Scholar](#)
53. Silver WL, Vogt KA (1993) Fine-root dynamics following single and multiple disturbances in a subtropical wet forest ecosystem. *J Ecol* 81:729–738[CrossRef](#)[Google Scholar](#)
54. Silver WL, Lugo AE, Keller M (1999) Soil oxygen availability and biogeochemistry along rainfall and topographic gradients in upland wet tropical forest soils. *Biogeochemistry* 44:301–328. doi: [10.1023/A:1006034126698](https://doi.org/10.1023/A:1006034126698)[Google Scholar](#)
55. Silver WL, Liptzin D, Almaraz M (2013) Soil redox dynamics and biogeochemistry along a tropical elevation gradient. In: Gonzalez G, Willig MR, Waide RB (eds) *Ecological gradient analyses in a tropical landscape*. Wiley, Hoboken[Google Scholar](#)
56. Sinsabaugh RL (2010) Phenol oxidase, peroxidase and organic matter dynamics of soil. *Soil Biol Biochem* 42:391–404[CrossRef](#)[Google Scholar](#)

57. Sutton-Grier AE, Keller JK, Koch R et al (2011) Electron donors and acceptors influence anaerobic soil organic matter mineralization in tidal marshes. *Soil Biol Biochem* 43:1576–1583. doi: [10.1016/j.soilbio.2011.04.008](https://doi.org/10.1016/j.soilbio.2011.04.008)[CrossRefGoogle Scholar](#)
58. Teh YA, Silver WL, Scatena FN (2009) A decade of belowground reorganization following multiple disturbances in a subtropical wet forest. *Plant Soil* 323:197–212. doi: [10.1007/s11104-009-9926-z](https://doi.org/10.1007/s11104-009-9926-z)[CrossRefGoogle Scholar](#)
59. Thompson A, Chadwick OA, Boman S, Chorover J (2006) Colloid mobilization during soil iron redox oscillations. *Environ Sci Technol* 40:5743–5749. doi: [10.1021/es061203b](https://doi.org/10.1021/es061203b)[CrossRefGoogle Scholar](#)
60. Thompson A, Rancourt D, Chadwick O, Chorover J (2011) Iron solid-phase differentiation along a redox gradient in basaltic soils. *Geochim Cosmochim Acta* 75:119–133. doi: [10.1016/j.gca.2010.10.005](https://doi.org/10.1016/j.gca.2010.10.005)[CrossRefGoogle Scholar](#)
61. Tonneijck FH, Jansen B, Nierop KGJ et al (2010) Towards understanding of carbon stocks and stabilization in volcanic ash soils in natural Andean ecosystems of northern Ecuador. *Eur J Soil Sci* 61:392–405. doi: [10.1111/j.1365-2389.2010.01241.x](https://doi.org/10.1111/j.1365-2389.2010.01241.x)[CrossRefGoogle Scholar](#)
62. Torn MS, Trumbore SE, Chadwick OA et al (1997) Mineral control of soil organic carbon storage and turnover. *Nature* 389:170–173. doi: [10.1038/38260](https://doi.org/10.1038/38260)[CrossRefGoogle Scholar](#)
63. Varela E, Tien M (2003) Effect of pH and oxalate on hydroquinone-derived hydroxyl radical formation during brown rot wood degradation. *Appl Environ Microbiol* 69:6025–6031. doi: [10.1128/AEM.69.10.6025-6031.2003](https://doi.org/10.1128/AEM.69.10.6025-6031.2003)[CrossRefGoogle Scholar](#)
64. Viollier E, Inglett P, Hunter K et al (2000) The ferrozine method revisited: Fe(II)/Fe(III) determination in natural waters. *Appl Geochem* 15:785–790. doi: [10.1016/S0883-2927\(99\)00097-9](https://doi.org/10.1016/S0883-2927(99)00097-9)[CrossRefGoogle Scholar](#)
65. Vogt KA, Vogt DJ, Palmiotto PA et al (1996) Review of root dynamics in forest ecosystems grouped by climate, climatic forest type and species. *Plant Soil* 187:159–219. doi: [10.1007/BF00017088](https://doi.org/10.1007/BF00017088)[CrossRefGoogle Scholar](#)
66. Wagai E, Mayer L (2007) Sorptive stabilization of organic matter in soils by hydrous iron oxides. *Geochim Cosmochim Acta* 71:25–35. doi: [10.1016/j.gca.2006.08.047](https://doi.org/10.1016/j.gca.2006.08.047)[CrossRefGoogle Scholar](#)

67. Wagai R, Mayer LM, Kitayama K, Shirato Y (2011) Association of organic matter with iron and aluminum across a range of soils determined via selective dissolution techniques coupled with dissolved nitrogen analysis. *Biogeochemistry* 112:95–109. doi: [10.1007/s10533-011-9652-5](https://doi.org/10.1007/s10533-011-9652-5)[CrossRef](#)[Google Scholar](#)
68. Weaver PL, Medina E, Pool D et al (1986) Ecological Observations in the Dwarf Cloud Forest of the Luquillo Mountains in Puerto Rico. *Biotropica* 18:79–85. doi: [10.2307/2388367](https://doi.org/10.2307/2388367)[CrossRef](#)[Google Scholar](#)